An innovative controller for optimal operation of Hybrid Energy Storage Systems

Federico Bianchi*, Enrica Micolano*, Luigi Pellegrino*, Alessio La Bella†, Guido Coletta‡, Domenica Maria Conenna§, Elisa Virone§, Giorgio Maria Giannuzzi‡, Cosimo Pisani‡

*Department of Generation Technologies and Material,
Ricerca sul Sistema Energetico S.p.A., Milan, Italy
Email: [federico.bianchi, enrica.micolano]@rse-web.it, ing.pellegrinoluigi@gmail.com

†DEIB, Politecnico di Milano, Milan, Italy
Email: alessio.labella@polimi.it

‡Power System Engineering, Terna Rete Italia, Rome, Italy
Email: {guido.coletta, giorgio.giannuzzi, cosimo.pisani}@terna.it

§Innovation Factory System Operator, Terna S.p.A., Rome, Italy
Email: [domenicamaria.conenna, elisa.virone]@terna.it

***Abstract*—Hybrid Energy Storage Systems (HESS) combine different energy storage technologies to maximize the contribution of each technology according to their own capability. Control schemes for the operation of such plants can reach high complexity level due to heterogeneity of lower control schemes and to the definition of proper control strategies for each technology. In this paper, an innovative controller for optimal operation of HESS is presented which combines virtualisation and optimisation algorithms to allow the aggregated control of the several Storage Units as an Equivalent Storage Unit. The controller is applied to Italian TSO Terna's Storage Lab facility in Codrongianos (Sardinia, Italy), an experimental 8 MW HESS plant connected to High Voltage grid which provides ancillary services. Preliminary results on simulated environment are presented.**

Keywords—hybrid energy storage system, BESS, energy management system, EMS, virtualization, optimization, grid ancillary services

I. INTRODUCTION

The energy sector is facing a transformation due to the widespread adoption of non-programmable renewable energy sources like wind and solar power. At the same time, there is a growing demand for electricity due to the electrification of various facilities, homes, and vehicles. This transition poses challenges to grid stability as maintaining a balance between electricity demand and generation becomes more complex. Conventional large-scale power plants that rely on inertia, such as gas and hydro plants, may not be sufficient to provide the flexibility required for a secure and reliable grid operation. Therefore, additional sources of flexibility are needed.

Energy Storage System (ESS) technologies have been introduced in power systems to address the intermittency of renewable generation and align it with electricity demand [1]. In addition to storing and smoothing renewable power, ESSs can enhance the resilience and efficiency of power system operation and planning, providing auxiliary services such as energy time shifting, peak shaving, and frequency regulation. Different ESS technologies have unique characteristics [2], in terms of *e.g.,* energy and power rating, energy and power density, response time, round-trip efficiency, and life cycle, but no single technology can fulfil all requirements asked for certain ESS applications. To overcome this, Hybrid Energy Storage Systems (HESS) combine multiple ESS technologies to leverage their individual strengths while mitigating limitations. This approach expands the range of advantages and enhances capabilities without requiring developments of the technology. Hybridization may happen either at system, device, or material level, providing technical and economic advantages beyond any single ESS, also considering sustainability and reliability of the hybridized solution. HESSs appear in both private (road) and public (rail) electric transport applications that require ESSs featuring high peak power and high energy density to cope with different driving modes [3]. Another situation which mandates the use of HESSs is in renewable energy where a HESS aids integration of intermittent renewable sources into the grid (or micro-grid) by providing long term energy balancing, short term power quality and frequency regulation services [4] [5]. Finally, service stacking, also known as value stacking or revenue stacking, is a promising and relevant approach for HESSs. By combining the best characteristics of each technology, it is possible to enhance the service portfolio the system can offer, thus accounting for various time horizons, combining short-term storage with seasonal or long-term storage capabilities.

Apart from few exceptions, as the HESS pilot plants reported in [6], the research on HESS technology is stagnant on laboratory scale with only theoretical perspective. Also, the proposed couplings are generally limited to two different technologies, the supercapacitor-battery, fuel cell-battery, fuel cell-supercapacitor, battery-flywheel, and fuel cell-flywheel HESS are commonly adopted coupling.

To effectively utilize HESS, well-designed Energy Management Systems (EMSs) are necessary. Typically, individual control systems are implemented for each individual ESS in HESS, often developed by different industrial partners, requiring coordination. Various architecture and control strategies have been analysed and developed for ESSs in recent years, [7] [8]. These strategies can be categorized into EMSs based on (i) supervisory control, (ii) operating time platform, and (iii) decision making approach. Belonging to the third category, Model Predictive

978-88-87237-60-3

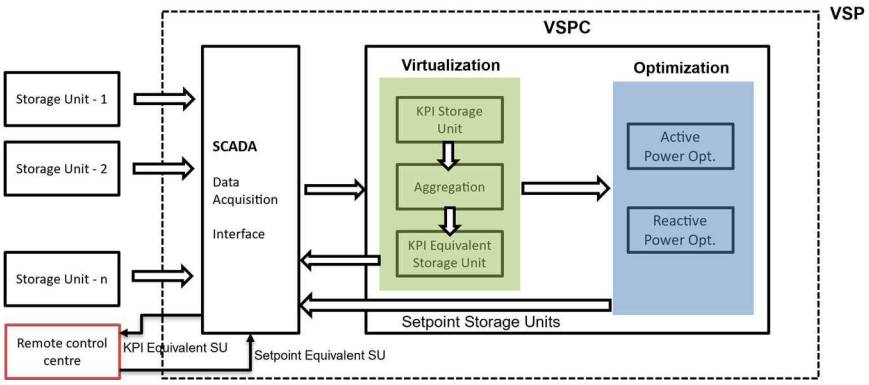

Fig. 1. Schematic representation of the proposed control and monitoring system.

Control (MPC) strategy is one of the most adopted and effective since it has the advantage of being able to account also for the degradation of the ESSs, which is a crucial aspect in all (H)ESS applications. It is to be noted that current EMS, even if based on MPC, are not designed for HESS but rather for simpler cases, such as combining a stationary battery with an electric vehicle.

This paper introduces a newly developed EMS called the Virtual Storage Plant (VSP) for HESS. It consists of different functional modules aiming at controlling and monitoring the different ESSs, also optimizing overall operation through innovative algorithms of *virtualisation* (aggregation and virtualisation of different ESSs, simplifying switching and dispatching activities) and *dynamic optimization* (integrating the model of each technology to provide real-time system optimization as minimizing battery aging). VSP implements simplified models of different ESSs to be used in the optimization process, such as circuital models, topology of the ESS, ageing rate, State-Of-Charge (SOC) estimators. The VSP is deployed on the hybrid energy storage plants owned by Terna, the Italian Transmission System Operator (TSO). The plants are equipped to provide ancillary services to support High Voltage (HV) grid stability.

The rest of the paper is organized as follows. Section 2 introduces the considered case study. Section 3 provides an overview of the control system being discussed and delves into the innovative algorithms of virtualization and optimization in more detail. Section 4 presents some results followed by concluding remarks in Section 5.

II. Case Study

Terna started the investigation on ESS [9]with Energy Intensive projects in 2011 and Power Intensive projects in 2012. The Power Intensive pilot project or *Storage Lab* is installed in two HV Terna substations located in the two main Italian islands, Sardinia and Sicily, with an overall size of 16 MW. The objective of Storage Lab is the assessment of the performances of different energy storage technologies in providing grid ancillary services [10]. Focusing on Sardinian site, within the 150kV HV substation of Codrongianos, Terna installed different technologies of Li-ion Battery-ESS (BESS), Sodium Nickel-Cloride batteries (Zebra), flow battery and supercapacitor-based ESS [11]. Each ESS is about 1 MW while the overall installed power is 8.56 MW. ESS are operated and monitored by Terna remote control centres. Each ESS exchanges active power with HV grid to provide mainly Frequency Containment Reserves (FCR), automatic Frequency Restoration Reserves (aFRR), manual Frequency Restoration Reserves (mFRR, also called system balancing), and can also exchange reactive power to provide voltage regulation. Minimum and maximum active power contribution for FCR and aFRR can be manually set by the grid operator fixing an operational range of active power variation. Also, a function to optimally manage the SOC of each ESS has been implemented. All the ESS are equipped with individual control systems, aimed at the control and monitoring of the operation of each ESS. Also, there is a master control system at plant level designed for the management of multi-technological battery plants, whose description follows in the next section.

III. Control System

Fig. 1 reports a schematic representation of the proposed control and monitoring system. Its main purpose is to manage multiple Storage Units (SUs) as a single Equivalent Storage Unit (ESU) to ensure coordinated management. The system includes a Supervisory Control and Data Acquisition (SCADA) module that acts as an interface between the SUs and the control room. The VSP Controller (VSPC) consists of data acquisition, virtualization, and optimization modules. VSPC receives input from the SCADA, monitors the system's status, and optimally dispatches the SUs. The virtualization module, inside the VSPC, defines aggregation logics to evaluate Key Performance Indicators (KPIs) of the ESU from those of the individual SUs. These indicators are also used by the optimizer to determine the optimal management strategy for each SU. By solving an optimization problem, the optimizer dispatches set-points among the SUs to collectively provide required services while minimizing individual SU aging.

The data acquisition, virtualization and optimization are indeed processes executed periodically. The VSPC utilizes a timed First-In-First-Out (FIFO) queue structure, where each process has its own queue. The queuing frequency of events depends on the specific process. The data acquisition process, responsible for reading SCADA data, is queued frequently according to the SCADA data refresh rate. In contrast, the virtualization and optimization processes have longer time intervals. The accurate selection of time intervals allows for achieving a VSP that is synchronous with the physical system, necessary for real-time state monitoring and optimal control.

A. Virtualization

The virtualization receives measurements including voltage, current, SOC of each SU, as well as the active and

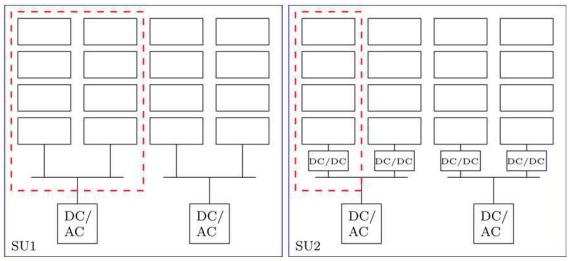

Fig. 3. Example of sub-system definition. The red (dashed) line denotes a sub-system.

reactive power of each Power Conversion System (PCS) and the status of switches, DC/DC or DC/AC converters present in each SU. Based on these, it returns (i) the SOC of the ESU, (ii) the maximum amount of energy that can be charged or discharged by the ESU at a given moment based on the required active power and current SOC (energy availability matrix), (iii) the maximum achievable active and reactive power of the ESU at a given moment (capability curve), and (iv) the State-of-Health (SOH) of the ESU and each SU. Here the SOH represents the ratio of the maximum energy that can be provided by the SUs and the ESU at a given moment compared to their nominal values.

To address the challenge of diverse manufacturers, technologies, and electrical configurations among the SUs, the concept of sub-systems (SS) is proposed. These sub-systems represent the smallest manageable subsets of each SU and allow for the estimation of state indicators to evaluate the SU's KPIs. Therefore, the SSs provide a standardized approach to handle the heterogeneity in SUs and assess their performance. As an example, consider the electrical configuration of two SUs reported in Fig. 3. The first SU consists of two PCS units connected to parallel strings, while the second has a separate DC/DC converter for each string. In SU1, the sub-system includes the two parallel strings, since managing a single string independently is not feasible, while in SU2, each string is treated as a separate sub-system.

The SOC of each SU is determined by (weighted) averaging the SOC of each SS that is connected to the grid and using the Voltage Dynamic-Based SOC Estimation (VDB-SE) algorithm [12], which estimates SOC and current maximum capacity based on open-circuit voltage curves. This approach is used instead of relying solely on the SOC measurement from the Battery Management System (BMS) due to potential unreliability. Additionally, the method allows for the estimation of SOH of the SUs. VDB-SE estimations is suitable for lithium-ion BESS except for Lithium iron phosphate (LFP), unless voltage or current measurements are unavailable, in which case the BMS SOC value is used. Formally, assuming N SUs,

$$SOC_{ESU} = \frac{\left(\sum_{i=1}^{N} SOC_i E_{n_i} \frac{C_i}{C_{n_i}}\right)}{\sum_{i=1}^{N} E_{n_i} \frac{C_i}{C_{n_i}}}, \qquad (1)$$

where E_{n_i} and C_i are the nominal SU energy and capacity, respectively, and C_i is the current SU capacity calculated as the sum of the SS capacities. The SOH of each SU is defined as:

$$SOH_i = \frac{\frac{C_i}{C_{n_i}} - p}{1 - p} 100, \qquad (2)$$

where $p \in [0,1]$ is the residual capacity in per unit corresponding to a null state of health (*i.e.,* end-of-life of the SU). Typical values are $p = 0.7$ or $p = 0.8$. Accordingly,

$$SOH_{ESU} = \frac{\sum_{i=1}^{N} SOH_i E_{n_i}}{\sum_{i=1}^{N} E_{n_i}} 100. \qquad (3)$$

The energy availability matrix represents the energy available in the SU based on varying power levels. The amount of energy considers battery models, conversion efficiency η, and SOC. The matrix values are derived by summing the available energy (State-of-Energy – SOE) from each SS, SOE_{SS}. The computation of each SOE_{SS} for a requested power P is depicted in Fig. 2. Firstly, the actual power required from the batteries P_b is determined, considering the specific charging, or discharging scenario. Then, the open-circuit voltage V_{OC_f} is evaluated to determine the voltage threshold at which the operational constraints (V_{min} or V_{max}) of the SS would be reached, according to the considered battery model. Hence, the open-circuit voltage curve is used to determine the final SOC, SOC_f. By knowing the initial and final SOC values, the SOE of the SS is calculated by multiplying the allowable SOC variation with the maximum energy of the SS, E. Please note that the open-

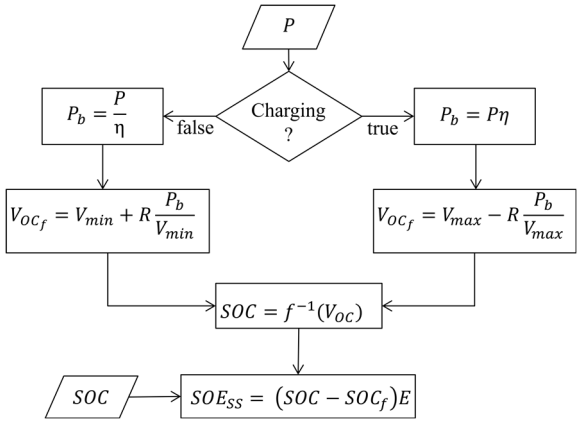

Fig. 2. Sub-system State-of-Energy (SOE_{SS}) computation.

circuit voltage curve $V_{OC} = f(SOC)$, as well as the efficiency η and the internal resistance R can be computed through dedicated experiments. Finally, the energy available in the i-th SU, for a given power request P, is given by:

$$E_i(P) = \sum_{j=1}^{N_{SS}} SOE_{SS_j}(P), \qquad (4)$$

where N_{SS} is the number of SS in the SU.

Now, based on (4), the maximum amount of energy that can be charged or discharged by the ESU at a given moment based on the required active power and current SOC can be computed. Assume that the power range of each SU is divided in K intervals equally spaced in which the power is kept constant to $p_{i,k}$, where pedix i denotes the SU; at each interval is assigned a binary variable $\alpha_{i,k}$. Each entry of the energy availability matrix for the ESU can be computed as:

$$\begin{aligned} SOE_{ESU}(P) = \quad & \max_{\alpha_{i,k}} \sum_{i=1}^{N} E_i(p_i) \\ s.t. \quad & \sum_{k=1}^{K} \alpha_{i,k} \le 1 \quad \forall i \\ & \sum_{i=1}^{N} p_i \ge P \\ & p_i = \sum_{k=1}^{K} p_{i,k} \alpha_{i,k} \quad \forall i \end{aligned} \qquad (5)$$

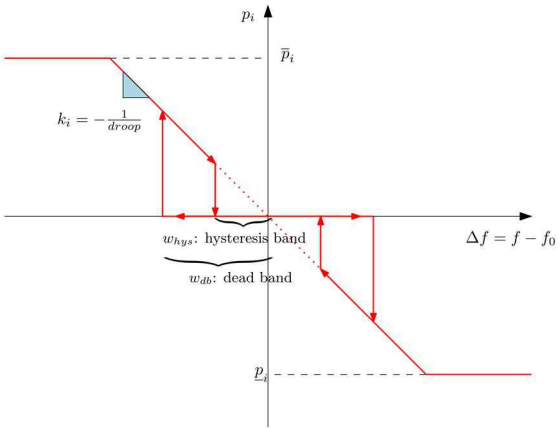

Fig. 4. Real FCR service for a SU. f_0 represents a nominal operating frequency.

where $E_i(p_i)$ is given by (4). Note that the first constraint imposes that each SU can contribute to satisfy the power request P with at most one power level $p_{i,k}$; the second constraint guarantees that the power request is accommodated.

Finally, the capability curve can be obtained from the ESU energy availability matrix. The capability represents the range of active power P_{ESU} within which the ESU can operate without violating the operational limits of the SUs. For each SU, the available apparent power A_i is calculated as the product of the SU's nominal power P_{n_i} and its state $s_i \in [0,1]$ which accounts for the number of active SSs in the SU. Accordingly,

$$A_{ESU} = \sum_{i=1}^{N} A_i = \sum_{i=1}^{N} P_{n_i} s_i. \qquad (6)$$

Assuming a circular capability, the reactive power is given by:

$$Q_{ESU} = \sqrt{A_{ESU}^2 - P_{ESU}^2}\,. \qquad (7)$$

Please note that, besides the number of active SSs in the SU, being storage systems, the capability also depends on both the SOC and the SOH.

B. Optimization

The optimization process involves distributing the desired set-point among different SUs within the ESU to ensure that the overall services requested to the equivalent unit are provided while minimizing the loss of energy capacity (the aging) of the individual SUs. For each SU, ancillary services can be provided either individually (*i.e.,* one service a time) or simultaneously (*i.e.,* service stacking mode) using a priority index to allocate the SU's capability among the activated services. For example, system balancing (mFRR) may take precedence over FCR and aFRR. Also, the so called "SOC objective" operating mode enables the system to achieve a desired SOC level while deactivating the provision of services. The resulting optimization problem is solved within the Model Predictive Control (MPC) framework. This control strategy involves periodically solving the optimization, considering a limited number of future time instances. By using mathematical models of the system dynamics, MPC predicts the future behaviour of the controlled system based on the chosen control action. This approach ensures adherence to operational constraints and optimal system management, even for future instances. In the following, the considered system dynamics, constraints, and cost terms are presented. At first, only FCR, aFRR, and mFRR services are considered.

The FCR service enables the SU to react to frequency variation, contributing to restore the balance between power generation and consumption in the grid. The power contribution is tailored according to the deviation in frequency from the nominal condition f_0 and the SU's droop value k_i, as shown in Fig. 4. The service is hence fully characterized by the parameters $\left(\overline{p}_i^{FCR}, \underline{p}_i^{FCR}, k_i, w_{db}, w_{hys}\right)$ for each SU. Accordingly, from a purely optimization standpoint, when considering the provision of the FCR service, each SU can be represented by its (simplified) power response to frequency changes, as depicted in Fig. 5 (a). Based on this model, the optimization defines for each SU the set-point $\left(\overline{p}_i^{FCR}, \underline{p}_i^{FCR}, k_i\right)$ – these are optimization variables – to fulfil the overall request by the system operator, *i.e.*, $\left(\overline{P}_{ESU}^{FCR}, \underline{P}_{ESU}^{FCR}, k_{ESU}\right)$, as graphically shown in Fig. 5 (b). Note that the frequency values f_l and f_u are assumed fixed and equal for all SUs, as well as the bands w_{db} and w_{hys}. Formally, for each SU the provided FCR power is defined as:

$$p_i^{FCR}(t) = \begin{cases} \overline{p}_i^{FCR}(t), & k_i(t)\Delta f(t) \geq \overline{p}_i^{FCR}(t) \\ \underline{p}_i^{FCR}(t), & k_i(t)\Delta f(t) \leq \underline{p}_i^{FCR}(t) \\ 0, & -w_{db} \leq \Delta f(t) \leq w_{db} \\ k_i(t)\Delta f(t) & otherwise \end{cases}, \qquad (8)$$

whereas the FCR parameters are constrained to satisfy:

$$\begin{aligned} \textstyle\sum_{i=1}^{N} \overline{p}_i^{FCR}(t) &= \overline{P}_{ESU}^{\mathrm{FCR}}(t) \\ \textstyle\sum_{i=1}^{N} \underline{p}_i^{FCR}(t) &= \underline{P}_{ESU}^{\mathrm{FCR}}(t)\,. \\ \textstyle\sum_{i=1}^{N} k_i(t) &= k_{ESU}(t) \end{aligned} \qquad (9)$$

The aFRR service is based on modulating the power generation in proportion to a reference signal $z(t) \in [0,1]$, ($z = 1$ stands for maximum power, $z = 0$ for minimum power, and $z = 0.5$ for no power variation) provided by the centralized automatic frequency regulator, with the aim of restoring the grid frequency to its nominal value. Assuming a symmetric regulation band for this service, the SU aFRR power can be modelled as:

$$p_i^{aFRR}(t) = \overline{p}_i^{aFRR}(t)(2z(t) - 1), \qquad (10)$$

where $\overline{p}_i^{aFRR}$ represents an optimization variable. This leads to the following aggregated constraints:

$$\begin{aligned} \textstyle\sum_{i=1}^{N} \overline{p}_i^{aFRR}(t) &= \overline{P}_{ESU}^{aFRR}(t) \\ \textstyle\sum_{i=1}^{N} \underline{p}_i^{aFRR}(t) &= \underline{P}_{ESU}^{aFRR}(t) \end{aligned}. \qquad (11)$$

With the purpose of addressing load or generation fluctuations resulting from one or multiple contingencies, the mFRR permits the injection of a power setpoint that deviates from the scheduled one according to an exogeneous control signal $r(t)$ sent by the operator. The SU mFRR power can be thus modelled as:

$$p_i^{mFRR}(t) = \alpha_i^{mFRR}(t) r(t), \qquad (12)$$

imposing that:

$$\begin{aligned} &0 \leq \alpha_i^{mFRR}(t) \leq 1 \\ &\textstyle\sum_{i=1}^{N} \alpha_i^{mFRR}(t) = 1' \end{aligned} \qquad (13)$$

to impose that the requested deviation is satisfied by the ESU.

Accordingly, the overall SU power is given by:

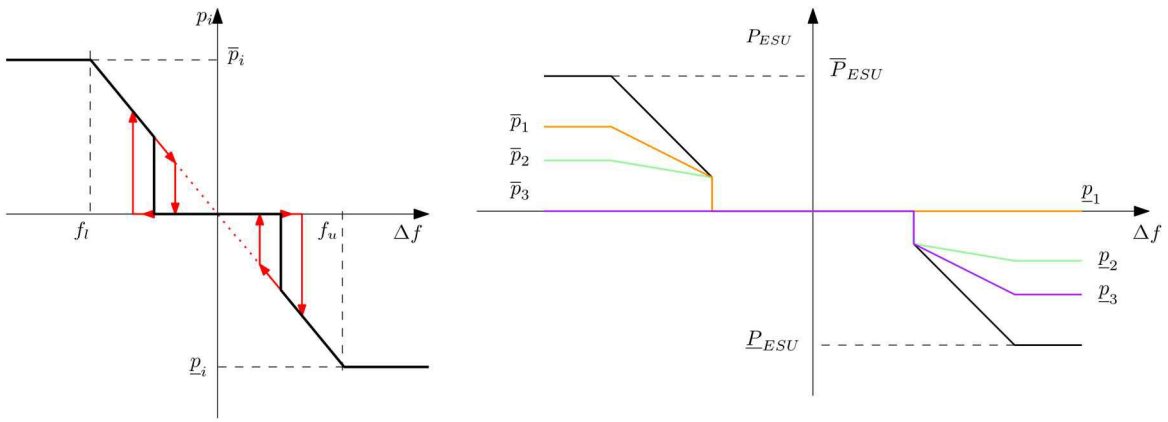

Fig. 5. FCR model. (a) Simplified model for a single SU (black line), (b) example of aggregation - ESU response (black line) and SUs' responses (colored lines).

$$p_i(t) = p_i^{FCR}(t) + p_i^{aFRR}(t) + p_i^{mFRR}(t). \quad (14)$$

A binary variable $\delta_{i,dch}$is introduced to distinguish between battery charging and discharging, leading to the following constraint:

$$p_i(t) \geq 0 \leftrightarrow \delta_{i,dch} = 1. \quad (15)$$

Furthermore, the power $p_i(t)$ is constrained by the SOE as:

$$p_i(t)\tau \leq E_i(p_i(t)), \quad (16)$$

where τ is the optimization interval period and $E_i(p_i)$ is given by (4). Recall that $E_i(p_i)$ in turn depends on the SOC dynamics:

$$SOC_i(t+1) = SOC_i(t) - \tau\, p_i(t)/C_n \quad (17)$$

as illustrated in Fig. 2. The SOC is always stays within a minimum $SOC_{min} > 0$ and a maximum value $SOC_{max} > 0$ and therefore:

$$SOC_{min} \leq SOC_i(t) \leq SOC_{max}. \quad (18)$$

Finally, the power $p_i(t)$ is constrained by the available capability as:

$$|p_i(t)| \leq A_i, \quad (19)$$

where A_i is the apparent power defined in (6) and the absolute value accounts for the charging and discharging battery status.

As introduced, the provision of ancillary services is allowed if and only if SOC_{ESU} stays within a desired range:

$$|SOC_{ESU}(t)| \leq SOC^{\circ} + th_{SOC}, \quad (20)$$

where SOC° is the SOC target and th_{SOC} is a threshold. Practically, constraint (20) is relaxed to allow for possible small violations $\xi_{SOC}(t)$ (they are optimization variables), which are penalized in the objective function by the cost term:

$$J_{SOC} = \sum_{t=1}^{T}\left(\xi_{SOC}(t)\right)^2. \quad (21)$$

Lastly, aging is accounted for by the cost term:

$$J_{age} = \sum_{t=1}^{T}\sum_{i=1}^{N}\left(a_i^{FCR}\left(\overline{p}_i^{FCR}(t) - \underline{p}_i^{FCR}(t)\right) + a_i^{aFRR}\overline{p}_i^{aFRR}(t) + a_i^{mFRR}p_i^{mFRR}(t)\right), \quad (22)$$

where a_i^{FCR}, a_i^{aFRR}, and a_i^{mFRR} are service dependent aging coefficients that can be estimated, for each SU, by dedicated experiments (see Table 2 where Li stands for lithium ion BESS and SC for supercapacitor-based ESS). The list of experiments done to get the parameters in Table 2 is reported in [13]. The MPC control thus aims to minimize (21)-(22) subject to (8)-(20).

IV. Results

In this section some results are presented to show the functioning of the optimizer. Specifically, these results refer to a single MPC optimization over a prediction horizon of $T = 7$ steps with a sampling time of 2 minutes. To predict the system response, the frequency values over this horizon are needed: it is assumed that at $t = 3$ the nominal frequency $f_n = 50$ Hz is restored. Note that in a robustly interconnected power system like the Italian Transmission grid, it is reasonable to expect that frequency fluctuations, outside the deadband of the frequency control, typically endure for less than 5 minutes [14]. To easy the discussion, consider the case in which no SOC° is imposed. Table 1 reports the simulation case study set-up. In this paper only the results for the FCR service are discussed.

Table 1. Case study set-up

Measurements			***Service priority***	
Frequency	49.8	Hz	FCR	1
Voltage	150	kV	aFRR	2
$\boldsymbol{z(t)}$	100	%	mFRR	3
Desired Set-Points				
$\boldsymbol{SOC_{min}}$	10%			
$\boldsymbol{SOC_{max}}$	90%			
$\boldsymbol{w_{DB}}$	0.0250			
$\boldsymbol{\overline{P}_{ESU}^{FCR}}$	3.54 MW			
$\boldsymbol{\underline{P}_{ESU}^{FCR}}$	-3.54 MW			
$\boldsymbol{k_{ESU}}$	-1/0.05			
$\boldsymbol{\overline{P}_{ESU}^{aFRR}}$	0.70 MW			
$\boldsymbol{r}$	2.83 MW			

Fig. 6 reports the set-points that fulfil the requested service in term of band reserved to FCR. It can be observed how the cumulative effect of individual SU aligns with the overall request. A thorough examination of this figure reveals that the provision of the FCR service primarily relies on utilizing SUs with lower aging coefficients. Fig. 7 reports the allocation of FCR by the optimizer based on the set-point requested by the

TABLE 2. AGING COEFFICIENTS. THESE ARE SERVICE DEPENDENT COEFFICIENTS THAT CAN BE ESTIMATED, FOR EACH SU, BY DEDICATED EXPERIMENTS.

Service	*Storage Unit*						
	Li1	**Li2**	**Li3**	**Li4**	**Li5**	**Zebra**	**SC**
FCR	0.054	0.053	0.026	0.001	0.026	0.026	0
aFRR	0.008	0.023	0.018	0.001	0.018	0.018	1
mFRR	0.017	0.016	0.013	0.001	0.013	0.013	1

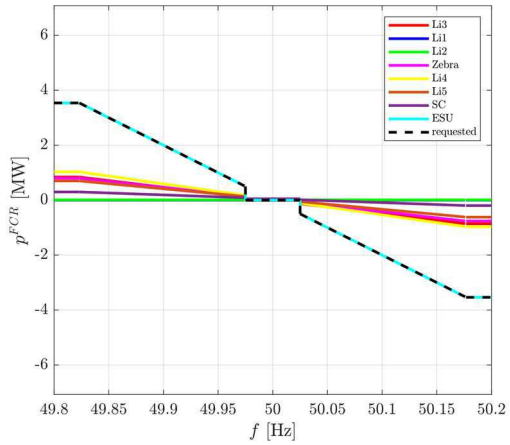

Fig. 6. Resulting FCR service for the first MPC step.

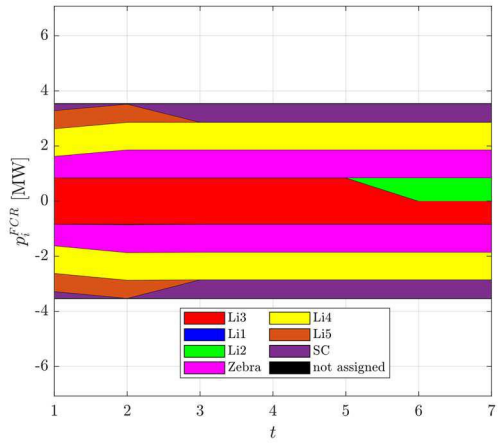

Fig. 7. Resulting FCR service power allocation.

system operator (see Table 1). The requested FCR reserve is guaranteed for the whole prediction horizon, exploiting the different storage units based on the aging coefficients in Table 2. For instance, the storage unit Li1, being one of the most subject to aging for the FCR service, is not exploited for the FCR service, whereas Li2 which is the second one most subject to aging, is just used at the end of the prediction horizon, as evident from Fig. 7.

V. CONCLUSION

This paper describes the VSP, an EMS properly designed for HESS with the scope of optimizing overall operation. The VSP is tested on the HESS of the Italian TSO Terna, sited in Codrongianos, a pilot plant equipped to provide ancillary services to support grid stability. The overall approach to the virtualisation technique and the optimisation problem as well as preliminary simulated test results are presented to clarify the operation of VSP. On-site testing carried out to validate the algorithms will be detailed in further studies. Terna is installing a Flywheel ESS that will allow further testing on the HESS control system. Also, grid forming algorithms will be implemented on one BESS, increasing the complexity of the HESS. Finally, with the aim of improving the estimation of ageing rate of ESSs, data-driven models could be developed by using training dataset from the operation of ESSs and integrated in the controller.

ACKNOWLEDGMENT

This work was partially funded by the Research Fund for the Italian Electrical System under the Three-Year Research Plan 2022-2024 (DM MITE n. 337, 15.09.2022), in compliance with the Decree of April 16th, 2018.

REFERENCES

[1] M. Beaudin, H. Zareipour, A. Schellenberglabe and W. Rosehart, "Energy storage for mitigating the variability of renewable electricity sources: An updated review," *Energy for Sustainable Development,* vol. 14, no. 4, pp. 302-314, 2010.

[2] S. Koohi-Fayegh and M. A. Rosen, "A review of energy storage types, applications and recent developments," *Journal of Energy Storage,* vol. 27, p. 101047, 2020.

[3] A. Khaligh and Z. Li, "Battery, ultracapacitor, fuel cell, and hybrid energy storage systems for electric, hybrid electric, fuel cell, and plug-in hybrid electric vehicles: State of the art," *IEEE transactions on Vehicular Technology,* vol. 59, no. 6, pp. 2806--2814, 2010.

[4] R. Hemmati and H. Saboori, "Emergence of hybrid energy storage systems in renewable energy and transport applications--A review," *Renewable and Sustainable Energy Reviews,* vol. 65, pp. 11--23, 2016.

[5] S. Hajiaghasi, A. Salemnia and M. Hamzeh, "Hybrid energy storage system for microgrids applications: A review," *Journal of Energy Storage,* vol. 21, pp. 543--570, 2019.

[6] T. S. Babu, K. Vasudevan, V. Ramachandaramurthy, S. B. Sani, S. Chemud and R. M. Lajim, "A comprehensive review of hybrid energy storage systems: Converter topologies, control strategies and future prospects," *IEEE Access,* vol. 8, pp. 148702--148721, 2020.

[7] P. Sharma, H. D. Mathur, P. Mishra and R. C. Bansal, "A critical and comparative review of energy management strategies for microgrids," *Applied Energy,* vol. 327, p. 120028, 2022.

[8] G. Chaudhary, J. Lamb, O. Burheim and B. Austbo, "Review of energy storage and energy management system control strategies in microgrids," *Energies,* vol. 14, no. 16, p. 4929, 2021.

[9] R. Benato, G. Bruno, F. Palone, R. Polito and M. Rebolini, "Large-scale electrochemical energy storage in high voltage grids: Overview of the Italian experience," *Energies,* vol. 10, no. 1, p. 108, 2017.

[10] R. Benato, S. Dambone Sessa, M. Musio, F. Palone and R. M. Polito, "Italian experience on electrical storage ageing for primary frequency regulation," *Energies,* vol. 11, no. 8, p. 2087, 2018.

[11] D. M. Conenna, M. G. Fadda, C. Boccarrato, F. Gasparotto and M. Pietrucci, "Features and functionalities of a supercapacitorbased storage system to support the Italian transmission grid," in *2020 AEIT International Annual Conference (AEIT)*, 2020.

[12] M. Mussi, L. Pellegrino, M. Restelli and F. Trovò, "A voltage dynamic-based state of charge estimation method for batteries storage systems," *Journal of Energy Storage,* vol. 44, p. 103309, 2021.

[13] Terna, "Rapporto di fine sperimentazione Stoage Lab," [Online]. Available: https://download.terna.it/terna/Rapporto_Pubblico_2015-2017_Power_8d91c5b5ae81739.pdf. [Accessed 13 09 2023].

[14] ENTSO-E, "Long Lasting Frequency Deviations Measures taken by Continental European TSOs to address Long Lasting Frequency Deviations," 2021.